Biosensors and Bioelectronics 32 (2012) 309–313

Contents lists available at SciVerse ScienceDirect

Biosensors and Bioelectronics

journal homepage: www.elsevier.com/locate/bios

Short communication

A cost-effective and field-ready potentiostat that poises subsurface electrodes to monitor bacterial respiration

Elliot S. Friedman[a], Miriam A. Rosenbaum[a,1], Alexander W. Lee[a,2], David. A. Lipson[b], Bruce R. Land[c], Largus T. Angenent[a,*]

[a] Department of Biological and Environmental Engineering, Cornell University, Ithaca, NY 14853, USA
[b] Department of Biology, San Diego State University, San Diego, CA 92182, USA
[c] School of Electrical and Computer Engineering, Cornell University, Ithaca, NY 14853, USA

ARTICLE INFO

Article history:
Received 29 October 2011
Received in revised form 6 December 2011
Accepted 8 December 2011
Available online 16 December 2011

Keywords:
Bioelectrochemical systems
Biosensing
Arctic peat soils
Microbial respiration
Potentiostat

ABSTRACT

Here, we present the proof-of-concept for a subsurface bioelectrochemical system (BES)-based biosensor capable of monitoring microbial respiration that occurs through exocellular electron transfer. This system includes our open-source design of a three-channel microcontroller-unit (MCU)-based potentiostat that is capable of chronoamperometry, which laboratory tests showed to be accurate within $0.95 \pm 0.58\%$ (95% Confidence Limit) of a commercial potentiostat. The potentiostat design is freely available online: http://angenent.bee.cornell.edu/potentiostat.html. This robust and field-ready potentiostat, which can withstand temperatures of $-30\,^{\circ}C$, can be manufactured at relatively low cost ($600), thus, allowing for *en-masse* deployment at field sites. The MCU-based potentiostat was integrated with electrodes and a solar panel-based power system, and deployed as a biosensor to monitor microbial respiration in drained thaw lake basins outside Barrow, AK. At three different depths, the working electrode of a microbial three-electrode system (M3C) was maintained at potentials corresponding to the microbial reduction of iron(III) compounds and humic acids. Thereby, the working electrode mimics these compounds and is used by certain microbes as an electron acceptor. The sensors revealed daily cycles in microbial respiration. In the medium- and deep-depth electrodes the onset of these cycles followed a considerable increase in overall activity that corresponded to those soils reaching temperatures conducive to microbial activity as the summer thaw progressed. The BES biosensor is a valuable tool for studying microbial activity *in situ* in remote environments, and the cost-efficient design of the potentiostat allows for wide-scale use in remote areas.

© 2011 Elsevier B.V. All rights reserved.

1. Introduction

Bioelectrochemical systems (BESs), including microbial fuel cells and microbial electrolysis cells, have been designed to utilize the ability of dissimilatory metal-reducing bacteria to respire with a solid-state electrode (Clauwaert et al., 2008; Cusick et al., 2011; Fornero et al., 2010; Hamelers et al., 2010; He et al., 2005; Liu et al., 2004; Lovley, 2006). In addition to waste treatment and energy or product recovery, BESs can be used as biosensors. Often for biosensor function, the working electrode (WE) is poised at a specific potential to mimic an electron acceptor (e.g., iron[III], humic acids) or an electron donor (e.g., iron[II]). This is accomplished with a microbial three-electrode system (M3C) for which the potential of a WE is controlled with respect to a reference electrode (RE). The current flowing into or out of the working electrode is measured via an equal and opposite current produced at the counter electrode (CE). A potentiostat is used to control the potential at the WE and to record the current. The resulting current produced by electrode-respiring bacteria can be directly linked to other parameters, including metabolic activity (Tront et al., 2008), biological oxygen demand (Chang et al., 2004; Kang et al., 2003), or biodegradable organic matter (Kumlanghan et al., 2007).

Currently, biosensing applications of BESs are limited by the price of potentiostats, which can cost up to $6000 per channel and are often unsuitable for long-term field use. Here, we present the design of an accurate, cost-effective, open-source, and field-ready potentiostat and demonstrate its use as a biosensor to study bacterial respiration in Arctic peat soils. Although other microcontroller-unit (MCU)-based potentiostats have been

* Corresponding author. Tel.: +1 607 255 2480; fax: +1 607 255 4449.
E-mail addresses: esf59@cornell.edu (E.S. Friedman), Miriam.Rosenbaum@rwth-aachen.de (M.A. Rosenbaum), awl9@cornell.edu (A.W. Lee), dlipson@sciences.sdsu.edu (David.A. Lipson), bruce.land@cornell.edu (B.R. Land), la249@cornell.edu (L.T. Angenent).
[1] Present address: Institute of Applied Microbiology, RWTH Aachen University, Worringer Weg 1, 52074 Aachen, Germany.
[2] Present address: The Boeing Company, Ridley Park, PA, USA.

0956-5663/$ – see front matter © 2011 Elsevier B.V. All rights reserved.
doi:10.1016/j.bios.2011.12.013

described in the literature for cyclic voltammetry (Gopinath and Russell, 2006), to the authors' knowledge, this is the first open-source design of an inexpensive potentiostat that is field ready for long-term chronoamperometry. We demonstrated the use of this MCU-based potentiostat as part of a fully-functional and stand-alone BES biosensor capable of operation in harsh environments (down to −30 °C) without electrical grid capabilities. The low cost of our open-source MCU-based potentiostat allows many to be employed across an ecosystem or as a sensor network; indeed, 24 potentiostatically-controlled BESs were deployed at different depths across four drained thaw lake basins around Barrow, AK. For at least five weeks, the WEs were poised at +0.1 V_{SHE} to mimic iron(III) compounds and humic acids; the resulting currents showed high variability across both drained thaw lake basin age and electrode depth. The most interesting results were the distinct increases in microbial respiration at deeper electrodes as the thaw progressed, indicating that elevated temperatures are stimulating microbial activity deeper into soils.

2. Experimental

2.1. Potentiostat design

2.1.1. Logical structure

The MCU-based potentiostat consists of four distinct parts: (i) the MCU (ATmega 644, Atmel, San Jose, CA), which serves as a central processing unit, distributing power and running all the other functions (additional information in S1.1, supplementary information); (ii) the secure digital (SD) card, which stores the gathered data; (iii) the user interface, which consists of an liquid crystal display (LCD) and push buttons; and (iv) the operational amplifier (op amp) circuitry, which provides the core of the potentiostat and interfaces between the MCU and the electrodes.

2.1.2. Hardware design

The electronic signal between the MCU and electrodes is processed by a series of op amps (Fig. 1), which is based on a previous MCU-based potentiostat by Gopinath and Russell (2006) and other basic potentiostat sources. The potential of the working electrode is applied in hardware from MCU output pins through a voltage divider and a 10 kΩ potentiometer. To apply the potential to the WE, the voltage of the RE is passed through a voltage follower (OA-1; Fig. 1), and then summed with the potential from the potentiometer so that the applied potential on the WE is with respect to the RE. To apply a negative potential, the potentiometer voltage is inverted with another op amp (OA-3; Fig. 1) before being applied to the WE. The voltage polarity can be switched by bypassing this op amp via a jumper located on the circuit board. The current entering the WE is measured through a corresponding current at the counter electrode, where it is converted to voltage through a current-to-voltage converting op amp (OA-4; Fig. 1). The feedback resistor (R) on the current-to-voltage converter sets the range of readable current (four choices: 200 μA; 400 μA; 1 mA; and 2 mA). The range is manually adjusted via a series of jumpers located on the circuit board. Since the internal ADC reads voltages between 0 and 1.1 V, the incoming voltage is shifted by half (550 mV) on the auxiliary board so that the range is centered around the origin (i.e., −500 μA to 500 μA in the 1 mA range) (OA-6; Fig. 1). This signal is read by the ADC input pins on the MCU and converted to a digital signal.

The user is able to set the time and WE potentials via the user interface, which consists of a LCD (Truly Semiconductors Ltd., Hong Kong) and four push buttons. In addition, the LCD allows the user to obtain real-time data for easy monitoring at the field site during operating periods. The LCD screen was designed on its own circuit board to allow it to be disconnected and stored between uses, since it cannot be left in extreme temperatures for extended operating periods.

2.1.3. Software design

Software was written in C using AVR Studio (Atmel, San Jose, CA) – this is included in the open source potentiostat design (additional information in S1.2, supplementary information). To minimize the impact of electronic noise from the MCU and the surrounding environment, recorded data points were averaged over fifty individual measurements taken within five milliseconds. The internal ADC converts the analog values to digital values, and the raw ADC input is converted to the appropriate current or applied potential. These values, along with the time of the measurement and operating parameters, are recorded to the SD card (Pretec, Taiwan).

2.2. Field location and experimental setup

Units were deployed at four different aged drained thaw lake basins – young (0–50 years), medium (50–300 years), old (300–2000 years), and ancient (3000–5000 years) – outside of Barrow, Alaska (Fig. 2a) (Hinkel et al., 2003). The medium-aged basin is located at the Biocomplexity Experiment in the Barrow Environmental Observatory and has AC power lines. However, the other sites do not have power lines. At each site we installed two potentiostats (eight total) with each potentiostat controlling three-electrode systems at each of three depths (7, 10, and 14 cm). Thus, we operated a total of 24 electrode systems. The three depths correspond to the aerobic, micro-aerobic, and anaerobic soil zones (Lipson et al., 2010). Potentials of +0.1 V_{SHE} were applied to the WE starting in late June (2011) to stimulate microbial respiration during an operating period of five to seven weeks. The soil temperature (5–10 cm below surface) was recorded every 30 min using a data logger (CR3000, Campbell Scientific, Logan, UT) with a temperature probe (Model 107, Campbell Scientific) at the medium-aged drained thaw lake basin (AC power available).

2.3. Electrode construction

For the WE and CE, 8 cm × 2.7 cm × 0.6 cm blocks were machined from medium-extruded graphite plates (Graphite Store, Buffalo Grove, IL), and 1.6129 mm holes were drilled in the top of the blocks. The exposed end of a 2.4 m length of 1.628 mm copper wire (ID Booth, Ithaca, NY) was tightly inserted into the hole and sealed using urethane adhesive (Ellsworth Adhesives, Germantown, WI) ($R \leq 0.5\ \Omega$). Electrodes were housed vertically in 5.1 cm polyvinyl chloride (PVC) piping with lengths of 7, 10, and 14 cm for shallow, medium, and deep electrodes, respectively (Fig. 2b).

Holes (2.7 cm × 0.6 cm) were drilled in 5.1 cm PVC knockout caps and the electrodes were affixed so that 6 cm of the electrode lengths were outside the piping, giving the electrodes a functional surface area of 41.2 cm^2. In the center of the 5.1 cm PVC piping, 1.3 cm PVC piping was inserted to allow the placement of a reference electrode (Ag/AgCl saturated KCl). The space between the 1.3 cm and 5.1 cm PVC tube was filled with a silica gel desiccant (Veritemp, Encino, CA), and the ends were sealed using urethane adhesive. Groups of three electrodes (shallow, medium, and deep) were held together using a hose clamp (Fig. 2b). Ag/AgCl saturated KCl reference electrodes were connected to 2.4 m lengths of copper wire similar to the other electrodes.

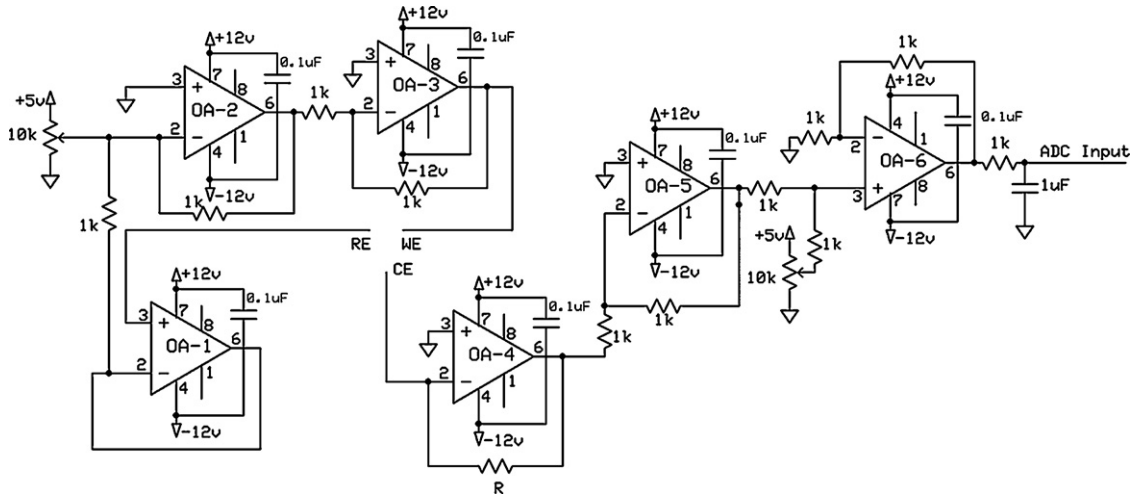

Fig. 1. Op amps (OA) that provide the core potentiostat circuitry. The working-electrode (WE) potential is poised with respect to the reference electrode (RE). The current necessary to maintain this potential is measured at the counter electrode (CE), and processed through a series of op amps before being read via analog-to-digital conversion. OA-3 inverts the applied potential to allow the application of a negative potential, and can be bypassed when a positive potential is required. A current-to-voltage conversion is performed at OA-4 through a precision resistor that sets the measurement range of the channel. The feedback resistor (R) for current-to-voltage conversion can be changed through a series of jumpers.

2.4. Field deployment

The potentiostats were housed in secure waterproof cases (Seahorse Cases, La Mesa, CA). A hole was drilled in the case for power, reference electrode, and electrode wires. The cases included desiccant packets (VeriTemp, Encino, CA) to prevent any moisture from damaging the electronics, and were locked to prevent tampering in the field. All external electrical connections were made using Buccaneer IP68 waterproof circular connectors (Bulgin, Essex, England).

AC power was used at the medium-aged site; 12 V power adapters (RS-15-12, TRC Electronics, Lodi, NJ) were added to the MCU-based potentiostats that were operated at this site. At the young-, old-, and ancient-aged sites, systems were powered using a combined solar panel-car battery system. A 20 W solar panel (BP Solar, Warrenville, IL) charged a 50 Ah deep cycle gel battery (Optima Batteries, Milwaukee, WI) (Fig. 2c). A solar controller (Morningstar Corporation, Newton, PA) regulated the current to the battery from the solar panel to prevent overcharging, and also controlled the power supply to the potentiostats. Each solar panel-battery system directly powered two potentiostats (i.e., six electrode systems).

3. Results & discussion

3.1. Lab tests of our MCU-based potentiostat

To ensure precision and accuracy, performance of the MCU-based potentiostat was compared against a commercial potentiostat (VSP, Biologic, Claix, France) using a resistor-capacitor (RC) circuit (Test Box #4, Biologic, Claix, France). This showed that our MCU-based potentiostat was accurate within $0.95 \pm 0.58\%$ (95% Confidence Limit) on the microamp scale throughout the 1 V operation range ($V_{WE} = -0.5$ to $0.5\ V_{REF}$) (Fig. S1).

3.2. A biosensor to study biogeochemical processes

Our BES biosensor is a valuable tool for environmental sensing, and can be used to aid the understanding of biogeochemical processes. The biosensor can be used in many different

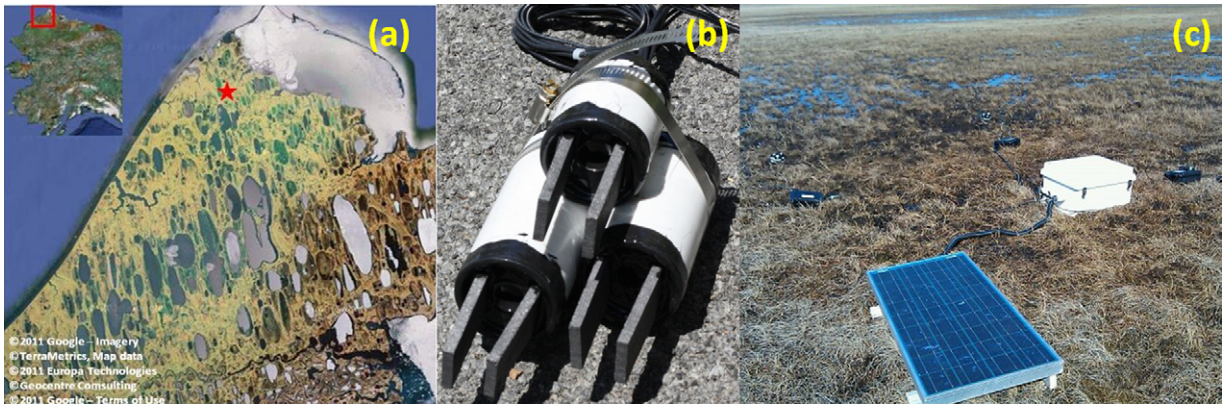

Fig. 2. Biosensing application in arctic peat soils: (a) Map of the area surrounding Barrow, AK where the subsurface biosensor was employed. The area of interested is denoted by a red box on a map of the entire state of Alaska (inset), and general area of research sites are denoted with a red star; (b) set of electrodes before being buried in the soil. There is a working and counter electrode at each of three depths (7 cm – top, 10 cm – bottom right, 14 cm – bottom left). The reference electrodes are inserted from the surface through a tube between the counter and working electrodes; and (c) MCU-based potentiostats with electrodes and solar panel-powered system deployed at a drained thaw lake basin. (For interpretation of the references to color in this figure legend, the reader is referred to the web version of the article.)

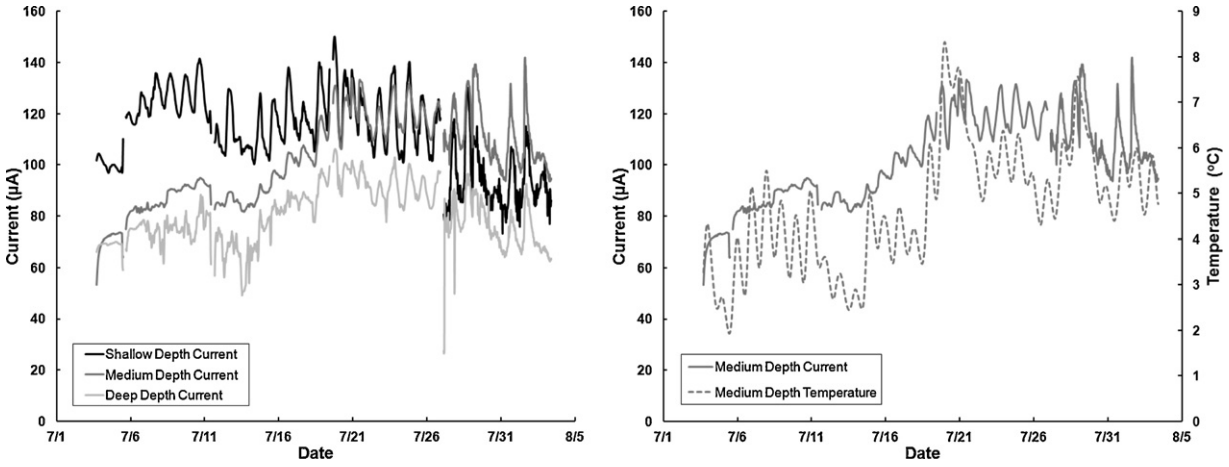

Fig. 3. Chronoamperometric data from potentiostatically-controlled system operated at an ancient-aged drained thaw lake basin: (a) the MCU-based potentiostat applied a potential of +0.1 V_{NHE} to working electrodes (WEs) at shallow (7 cm), medium (10 cm), and deep (14 cm) depths; and (b) the electric current at the medium-depth WE overlaid with soil temperature (5–10 cm probe depth located at the medium-aged site, which was one mile from the ancient-aged site). The increase in current production and onset of daily cycles corresponds to the increase in soil temperature between July 13th and July 20th.

environments. We tested our system with peat soils in the arctic (Fig. 2a and c). These soils are a major carbon reservoir (containing up to 1.7×10^{18} g (Tarnocai et al., 2009)); however, little is known about the underlying biogeochemistry and the effects that continued climate change will have on carbon stored in these dense and organic-rich soils (Allen et al., 2010; Bockheim et al., 2003; Oechel et al., 1995; Pastor et al., 2003; Schmidt et al., 2011; Tarnocai et al., 2009). Microbial processes are at the heart of the carbon cycle in peat soils, and small changes in environmental factors (e.g., temperature, pH, dissolved oxygen) can alter the dominance of microbial processes responsible for either CH_4 or CO_2 production (Hoj et al., 2008; Metje and Frenzel, 2007; Moore and Dalva, 1997). The reduction of iron(III) and humic acids via dissimilatory metal-reducing-like bacteria is a microbial process that competes with methanogenesis in the environment (Achtnich et al., 1995; Cervantes et al., 2002; Lovley et al., 1996; Lovley and Goodwin, 1988; Lovley and Phillips, 1987; Stams et al., 2006). The production of CH_4 with methanogens rather than CO_2 with dissimilatory metal-reducing-like bacteria has considerable impact on climate change because of the 21 times higher climate-forcing potential of CH_4 vs. CO_2. Iron(III) and humic acids are present in high concentrations in drained thaw lake basins that dominate Alaska's North Slope (Lipson et al., 2010). Therefore, a mechanistic understanding of the underlying biogeochemistry of these peat soils is crucial when predicting the long-term effects of climate change.

3.3. Field operation reveals weather-influenced subsurface microbial activity

We operated eight MCU-based potentiostats (24 channels) as *in-situ* biosensors in the field at four different sites for a period of five-seven weeks. At three sites, we operated them off-grid with solar panel-battery powered systems. Our 20 W photovoltaic systems at each site provided adequate power for the entire operating period (midnight-sun conditions), including at the ancient-aged drained thaw lake basin site for which we show data here (Fig. 3).

At the ancient-aged site, the electric current from our subsurface electrodes during the first 2–3 weeks of the operating period was higher for the shallow–depth electrode compared to the medium- and deep-depth electrodes (~100 μA compared to ~80 μA and ~70 μA, respectively) (Fig. 3a). Our system does not distinguish between electric current from abiotic and biotic reactions at the set potential; however, we anticipate that abiotic reactions are catalyzed without a lag period and then exist at a relatively constant rate controlled by the diffusion of oxidized redox species to the WE. On the other hand, for biotic reactions we observe lag periods to grow cells and a considerable sensitivity to temperature changes. For example, we have observed diurnal changes in electric current from pure cultures of *Geobacter sulfurreducens* in a microfluidic system that was not temperature controlled and that closely followed the daily temperature changes of our laboratory (data not shown). Here, we observe daily cycles of electric current, which were evident within a week at the shallow depth with daily maximums occurring between 15:00 and 18:00 and daily minimums occurring between 6:00 and 9:00. These cycles correlated closely to daily changes in soil temperature (a microbial growth parameter), which indicates that the electric current associated with these cycles is biotic. However, further experiments are necessary to ascertain the ratios of abiotic and biotic current responses. The diurnal electric current cycles became more distinct as the summer progressed.

Currents in the medium- and deep-depth electrodes, which were initially lower compared to the shallow–depth electrode, experienced an increase in average current during the third week of operation (July 13th–20th) to ~120 μA and ~90 μA, respectively (Fig. 3a). In addition, the daily cycles that were initially present only at the shallow–depth electrode became evident at the medium- and deep-depth electrodes following the July 13th–20th increase in electric current. This increase in current corresponded to an increase in medium-depth soil temperature of ~2 °C (Fig. 3b); prior to July 13th the average temperature was 3.66 ± 0.81 °C, while after July 20th the average temperature was 5.44 ± 0.71 °C. This correlation with our system indicates that microbial activity is limited by growth conditions and not by the availability of terminal electron acceptors (i.e., the electrode). This finding supports the theory that climate-driven increases in temperature could stimulate further increases in subsurface microbial activity, but only if enough natural electron acceptors are present in the soil.

By the end of the operating period, the average current with the medium-depth electrodes had surpassed the shallow–depth current. In addition, the current for the deep-depth electrode system was comparable to the shallow–depth electrode system (Fig. 3a). This indicates that the deeper and denser soils, which are richer in organic substrates, have the potential for higher microbial activity if they experience increased thaws.

This is another indication that continued climate change could unlock previously dormant carbon from tundra soils, although further investigation is necessary to fully comprehend these processes. We are planning to continue our monitoring in future years to

reveal the effects of climate change on these microbial communities. It is important to understand, however, that our biosensor systems are just one tool for research and that the electrochemical results must be correlated to many other environmental measurements and information from molecular biology tools to eventually predict the true impact of climate change on these fragile Arctic ecosystems.

3.4. Other possible biosensor applications for our MCU-based potentiostat

As increased monitoring of the environment is necessary to fully comprehend the effects of climate change; this potentiostatically-controlled BES provides a tool to monitor microbial activity *in situ* and in real time. Furthermore, it is a stand-alone, weather-proof system, allowing it to be deployed in remote areas with no existing infrastructure (i.e., electrical power, buildings). The design of the low-cost MCU-based potentiostat was essential to this application because it enabled biosensors to be deployed in large numbers (24 BESs) across a highly varied ecosystem. The MCU-based potentiostat has the potential for other applications, including *in situ* pollutant remediation and industrial process control.

The development of these biosensing systems are advantageous because they allow for real-time and *in-situ* monitoring, and could alleviate the need for time-intensive and laborious analysis methods. Furthermore, the design presented here could be easily augmented with additional features to improve usability with minimal additional hardware components; this could include wireless monitoring and control or the performance of additional electrochemical techniques (i.e., linear sweep voltammetry, cyclic voltammetry).

4. Conclusions

Here, we describe the design and operation of an accurate, field-ready, cost-effective, and MCU-based potentiostat and demonstrate its use as part of a novel subsurface BES-based biosensor. The field-ready MCU-based potentiostat is accurate within $0.95 \pm 0.58\%$ (95% Confidence Limit) of commercial potentiostats and can be manufactured for a fraction of the cost, enabling many systems to be utilized across a large area as *in-situ* biosensors. The potentiostatically-controlled BES presented functions as a standalone system, allowing for deployment in remote areas. The application of this system as a novel subsurface biosensor was demonstrated through its use in monitoring microbial respiration in Arctic peat soils. Daily cycles in microbial activity were evident, and results indicate that microbes in deeper soil layers became increasingly active as the soil temperature increased throughout the summer.

Acknowledgements

The authors would like to acknowledge Dr. Ted K. Raab and Eric Slessarev (Stanford University), Kim Miller (San Diego State University), and Jim Miller (Cleveland Heights High School) for assistance in conducting field work. This work was funded by the U.S. NSF Grant #0808604.

Appendix A. Supplementary data

Supplementary data associated with this article can be found, in the online version, at doi:10.1016/j.bios.2011.12.013.

References

Achtnich, C., Bak, F., Conrad, R., 1995. Biol. Fertil. Soils 19 (1), 65–72.
Allen, B., Willner, D., Oechel, W.C., Lipson, D., 2010. Environ. Microbiol. 12 (3), 642–648.
Bockheim, J.G., Hinkel, K.M., Nelson, F.E., 2003. Soil Sci. Soc. Am. J. 67 (3), 948–950.
Cervantes, F.J., de Bok, F.A.M., Tuan, D.D., Stams, A.J.M., Lettinga, G., Field, J.A., 2002. Environ. Microbiol. 4 (1), 51–57.
Chang, I.S., Jang, J.K., Gil, G.C., Kim, M., Kim, H.J., Cho, B.W., Kim, B.H., 2004. Biosens. Bioelectron. 19 (6), 607–613.
Clauwaert, P., Toledo, R., Van der Ha, D., Crab, R., Verstraete, W., Hu, H., Udert, K.M., Rabaey, K., 2008. Water Sci. Technol. 57 (4), 575–579.
Cusick, R.D., Bryan, B., Parker, D.S., Merrill, M.D., Mehanna, M., Kiely, P.D., Liu, G.L., Logan, B.E., 2011. Appl. Microbiol. Biotechnol. 89 (6), 2053–2063.
Fornero, J.J., Rosenbaum, M., Angenent, L.T., 2010. Electroanalysis 22 (7-8), 832–843.
Gopinath, A.V., Russell, D., 2006. Chem. Educ. 11 (1), 23–28.
Hamelers, H.V.M., Ter Heijne, A., Sleutels, T.H.J.A., Jeremiasse, A.W., Strik, D.P.B.T.B., Buisman, C.J.N., 2010. Appl. Microbiol. Biotechnol. 85 (6), 1673–1685.
He, Z., Minteer, S.D., Angenent, L.T., 2005. Environ. Sci. Technol. 39 (14), 5262–5267.
Hinkel, K.M., Eisner, W.R., Bockheim, J.G., Nelson, F.E., Peterson, K.M., Dai, X.Y., 2003. Arctic Antarct. Alpine Res. 35 (3), 291–300.
Hoj, L., Olsen, R.A., Torsvik, V.L., 2008. ISME J. 2 (1), 37–48.
Kang, K.H., Jang, J.K., Pham, T.H., Moon, H., Chang, I.S., Kim, B.H., 2003. Biotechnol. Lett. 25 (16), 1357–1361.
Kumlanghan, A., Liu, J., Thavarungkul, P., Kanatharana, P., Mattiasson, B., 2007. Biosens. Bioelectron. 22 (12), 2939–2944.
Lipson, D.A., Jha, M., Raab, T.K., Oechel, W.C., 2010. J. Geophys. Res. 115, G00I06.
Liu, H., Ramnarayanan, R., Logan, B.E., 2004. Environ. Sci. Technol. 38 (7), 2281–2285.
Lovley, D.R., 2006. Curr. Opin. Biotechnol. 17 (3), 327–332.
Lovley, D.R., Coates, J.D., BluntHarris, E.L., Phillips, E.J.P., Woodward, J.C., 1996. Nature 382 (6590), 445–448.
Lovley, D.R., Goodwin, S., 1988. Geochim. Cosmochim. Acta 52 (12), 2993–3003.
Lovley, D.R., Phillips, E.J.P., 1987. Appl. Environ. Microbiol. 53 (11), 2636–2641.
Metje, M., Frenzel, P., 2007. Environ. Microbiol. 9 (4), 954–964.
Moore, T.R., Dalva, M., 1997. Soil Biol. Biochem. 29 (8), 1157–1164.
Oechel, W.C., Vourlitis, G.L., Hastings, S.J., Bochkarev, S.A., 1995. Ecol. Appl. 5 (3), 846–855.
Pastor, J., Solin, J., Bridgham, S.D., Updegraff, K., Harth, C., Weishampel, P., Dewey, B., 2003. Oikos 100 (2), 380–386.
Schmidt, M.W.I., Torn, M.S., Abiven, S., Dittmar, T., Guggenberger, G., Janssens, I.A., Kleber, M., Kogel-Knabner, I., Lehmann, J., Manning, D.A.C., Nannipieri, P., Rasse, D.P., Weiner, S., Trumbore, S.E., 2011. Nature 478 (7367), 49–56.
Stams, A.J.M., de Bok, F.A.M., Plugge, C.M., van Eekert, M.H.A., Dolfing, J., Schraa, G., 2006. Environ. Microbiol. 8 (3), 371–382.
Tarnocai, C., Canadell, J.G., Schuur, E.A.G., Kuhry, P., Mazhitova, G., Zimov, S., 2009. Global Biogeochem. Cycles 2, 3.
Tront, J.M., Fortner, J.D., Plotze, M., Hughes, J.B., Puzrin, A.M., 2008. Biosens. Bioelectron. 24 (4), 586–590.